Nitrogen-based lung clearance index

Darquenne, Chantal; Theilmann, Rebecca J; Fine, Janelle M; Verbanck, Sylvia A B

Published in:
Journal of Applied Physiology (Bethesda, Md. : 1985)

DOI:
10.1152/japplphysiol.00511.2021

Publication date:
2022

License:
Unspecified

Document Version:
Accepted author manuscript

Nitrogen-based lung clearance index : a valid physiological biomarker for the clinic.

C. Darquenne[1*], R.J. Theilmann[2], J.M. Fine[1], and S. Verbanck[3].

[1]Dept. of Medicine, University of California, San Diego - La Jolla, CA (USA), [2]Dept. of Radiology, University of California, San Diego - La Jolla, CA (USA), [3] Vrije Universiteit Brussel (VUB), Universitair Ziekenhuis Brussel (UZ Brussel), Respiratory Division , Brussels, Belgium.

Corresponding author: Chantal Darquenne, PhD

Department of Medicine

University of California, San Diego

9500 Gilman Drive, mail code 0623A

La Jolla, CA 92093-0623

Email: cdarquenne@health.ucsd.edu

Author contributions: C.D. and S.V. designed the study; C.D., R.J.T. and J.M.F. collected the data.; C.D. analyzed the data. C.D. and S.V. drafted the manuscript. All authors edited and approved the final version of the manuscript.

Running title: N_2-based LCI as a meaningful physiological biomarker

ABSTRACT

Multiple breath washout (MBW) testing is increasingly used as a physiological measurement in the clinic, due in part to the availability of commercial equipment and reference values for MBW indices. Commercial N_2 washout devices are usually based on indirect measurement of N_2 concentration (C_{N2}), by directly measuring either molar mass and O_2 and CO_2, or molar mass and CO_2. We aim to elucidate the role of two potential pitfalls associated with N_2-MBW testing that could override its physiological content: indirect N_2 measurement and blood-solubility of N_2. We performed MBW in 12 healthy adult subjects using a commercial device ($MBW_{indirect}$) with simultaneous direct gas concentration measurements by mass spectrometry (MBW_{direct}) and compared C_{N2} between MBW_{direct} and $MBW_{indirect}$. We also measured argon concentration during the same washouts to verify the maximal effect gas solubility can have on N_2-based functional residual capacity (FRC) and lung clearance index (LCI). Continuous N_2 concentration traces were very similar for $MBW_{indirect}$ and MBW_{direct}, resulting in comparable breath-by-breath washout plots of expired concentration and in no significant differences in FRC_{N2}, LCI_{N2}, S_{cond} and S_{acin} between the two methods. Argon washouts were slightly slower than N_2 washouts, as expected for a less diffusive and more soluble gas. Finally, comparison between LCI_{N2} and LCI_{Ar} indicates that the maximum impact from blood-tissue represents less than half a LCI unit in normal subjects. In conclusion, we have demonstrated by direct measurement of N_2 and twice as soluble argon, that indirect N_2 measurement can be safely used as a meaningful physiological measurement.

New and noteworthy: The physiological content of N_2 multibreath washout testing has been questioned due to N_2 indirect measurement accuracy and N_2 blood solubility. With direct measurement of N_2 and twice as soluble argon, we show that these effects are largely outweighed by ease of use.

Keywords: Multiple breath washouts, nitrogen, lung clearance index

INTRODUCTION

Multiple breath washout (MBW) testing and derived lung clearance index (LCI) are increasingly being used as a physiological measurement in the clinic, due in part to the availability of commercial equipment, and to emerging reference values for N_2- and SF_6-based LCI (1, 2). The ease of implementing MBW in the clinic with ubiquitous availability of pure oxygen could be considered in favor of LCI measurement based on N_2 washout, but potential issues with N_2 measurement have led authors to promote the use of SF_6 instead (3). Comparative studies generally show functional residual capacity (FRC) which is smaller for SF_6 than for N_2 and an LCI for SF_6 that is either smaller or similar to LCI for N_2 (4-7). Four effects have been identified that potentially distinguish N_2 from SF_6 washout: (a) a more diffusive gas (i.e., N_2) washes out faster than a heavier less diffusive gas (i.e., SF_6) (8); (b) a blood-tissue soluble gas (i.e., N_2) contributes to the tail end of the washout (9-11); (c) an exogenous gas (i.e., SF_6) washed in prior to washout, may wash out faster because less ventilated lung units are at relatively lower initial concentration (12); (d) indirect gas measurement may generate an erroneous zero baseline (5, 6).

Currently, commercial N_2 washout devices are usually based on indirect measurement of N_2 concentration (C_{N2}), by directly measuring either molar mass and O_2 and CO_2, or molar mass and CO_2 (13). In an attempt to elucidate the role of two potential pitfalls associated with N_2-MBW testing, i.e., indirect N_2 measurement and blood-solubility of N_2, we compared C_{N2} from a commercial MBW device using molar mass and CO_2 measurement, with direct measurement by mass spectrometry. In addition, we measured argon concentration (C_{Ar}) during the same washout, because argon is also lung resident, has similar diffusion coefficient (factor ~1.2), but is

twice as soluble as N_2. This allowed us to verify the maximal effect gas solubility can have on N_2-based FRC and LCI.

METHODS

This study was approved by the University of California, San Diego's Human Subjects Research Protection Program. Subjects participated after giving written, informed consent.

MBW were performed in triplicate in 12 healthy adult subjects (6M/6F; age: 50±13(SD)yr) with 1-liter tidal breathing using a commercial device (EasyOne proLAB™, Wbreath 3.55, ndd MedizintechnikAG, Zurich, Switzerland) referred thereafter as $MBW_{indirect}$. Simultaneous direct gas concentration measurements (MBW_{direct}) were obtained by inserting a mass-spectrometer (Perkin-Elmer MGA1100, Pomona, CA) sampling line in the mouthpiece. Gas concentrations were acquired from the mass-spectrometer at 200 Hz using an analog-to-digital converter and dedicated computer software. Owing to the linear response of the mass-spectrometer (14), a two-point gas calibration was performed with 100% O_2 and a certified gas mixture of 9760ppm Ar, 4.99% CO_2, 16% O_2, balance N_2. N_2 concentration data from the commercial device is based on molar mass ultrasonic measurement and a CO_2 sensor; for the latter a correction is applied based on estimated O_2 concentration as described in the manufacturer documentation on the EasyOne Pro LAB Measurement Technology Background (15). The manual CO_2 gain option was used and set to gain = 1, thereby avoiding potential inaccuracies that can arise when using a respiratory-quotient-based adjustment of the CO_2 sensor (16). Flow and volume data were obtained from the commercial device. Gas concentration data from the commercial device and

the mass-spectrometer were aligned by matching tracings of CO_2 concentration (C_{CO2}) at 50% of the maximum C_{CO2} in the transition from expiration to inspiration as illustrated by the arrow in Figure 1. In doing so, concentration traces for N_2 were properly aligned throughout the washout, as can be appreciated from the example in Figure 2. Hence, it was not deemed necessary to attempt a correction for the potential impact of change in gas viscosity throughout the washout for the purpose of this study.

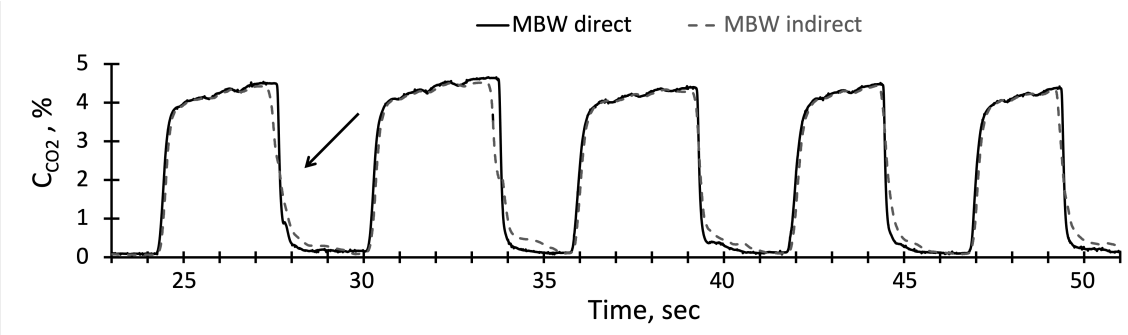

Figure 1. Alignment of gas concentration traces from the mass-spectrometer (MBW_{direct}) and the commercial device ($MBW_{indirect}$) by matching the C_{CO2} at 50% of maximal C_{CO2} in the transition from the first expiration of the MBW test to the next inspiration (see arrow).

Data analysis. Data were analyzed using WBreath v3.57 (NDD Medical Technologies, Switzerland) and code implemented in Matlab (Matlab R2020b, The Mathworks, Natick, MA). Mean expired and end-tidal gas concentrations were computed from flow and gas concentration data. FRC was determined from mass balance as the net volume of cumulative expired nitrogen down to the point where expired C_{N2} falls below 1/40 of initial end-tidal concentration divided by the difference between the initial and final concentrations of the gas. LCI was calculated from mean expired C_{N2}, end-tidal C_{N2} and also from mean expired C_{Ar}, where the intercept with the $1/40^{th}$ level was determined by linear regression of the concentrations versus turnover (TO) on the two breaths before and after that at which concentration falls below the $1/40^{th}$ line. We also

quantified the continuing rate of FRC increase at the $1/40^{th}$ level of pre-test end-tidal concentration as a means to assess the continued effect of gas stored in blood and tissues on MBW indices at the washout level where LCI is determined. This was done by a regression of FRC versus time on the two breaths before and two breaths after the $1/40^{th}$ level. Finally, indices of acinar (S_{acin}) and conductive (S_{cond}) ventilation heterogeneity were derived from an alveolar slope analysis of both $MBW_{indirect}$ and imported MBW_{direct} N_2 concentration trace (17).

To help understand the experimental results, we also determined the breath-by-breath nitrogen dilution of a perfectly mixed gas with an initial C_{N2} at 78% during 100% O_2 1L tidal breathing in a 3L two–compartment lung model without any dead space. A 40% and 55% partitioning of respectively FRC and tidal volume (VT) was introduced to produce a specific ventilation or turnover of one compartment (55%VT/40%FRC = 1.38 VT/FRC) almost twice that of the other one (45%VT/60%FRC= 0.75 VT/FRC), typical of ventilation distribution between gravity-dependent upper and lower lung regions. Breath duration was 4s and soluble gas excretion rate was that provided by Lundin (18) for N_2 (i.e., $37.3*e^{(-0.45\ t)} + 13.9\ e^{(-0.056*t)} + 4.82\ e^{(-0.0054*t)}$ where t is time expressed in minutes).

Statistical analysis. All data are expressed as means ± SD. Paired-student's t-test was used to evaluate the difference between MBW_{direct}- and $MBW_{indirect}$-derived FRC, LCI, S_{cond} and S_{acin} measurements, and also to evaluate the difference between MBW indices derived from nitrogen and argon gas concentrations. Significance was accepted at $P < 0.05$, two-tailed.

RESULTS

Continuous N_2 concentration traces were very similar for $MBW_{indirect}$ and MBW_{direct} (Figure 2a), resulting in comparable breath-by-breath washout plots of mean expired (Figure 2b) or end-tidal N_2 concentration (Figure 2c). In addition, mean expired argon washouts were slightly slower than mean expired N_2 washouts, as expected for a less diffusive and more soluble gas. It should be noted that, although argon tracings were noisier than that of N_2, the signal-to-noise ratio (SNR) was still high enough to provide meaningful results. Indeed, the SNR at an argon concentration of 0.976 (i.e., at the start of the MBW) was 1:180 and dropped to 1:5 at $1/40^{th}$ of the starting argon concentration, a SNR value still above 3, i.e., the typical threshold value for detectable signals.

There were no significant differences in FRC_{N2} (average$\pm$SD) measured with MBW_{direct} (2.74 ± 0.67 L) or with $MBW_{indirect}$ (2.70 ± 0.70 L; p=0.3) (Figure 3a). The same was true when comparing LCI_{N2} computed from mean expired C_{N2} (MBW_{direct}: 6.09 ± 0.43 vs. $MBW_{indirect}$: 6.02 ± 0.36; p=0.3) (Figure 3b) or from end-tidal C_{N2} (MBW_{direct}: 6.74 ± 0.53 vs. $MBW_{indirect}$: 6.63 ± 0.39; p=0.6) (Figure 3c). There were no significant differences in S_{cond} (Figure 3d) and S_{acin} (Figure 3e) derived from MBW_{direct} or $MBW_{indirect}$ N_2 traces (S_{cond}: 0.033 ± 0.015 L^{-1} for MBW_{direct} vs. 0.032 ± 0.016 L^{-1} for $MBW_{indirect}$, p=0.1; S_{acin}: 0.089 ± 0.056 L^{-1} for MBW_{direct} vs. 0.092 ± 0.054 L^{-1} for $MBW_{indirect}$, p=0.5). Considering the more soluble argon, FRC_{Ar} was 2.87±0.69 L and LCI for mean expired C_{Ar} was 6.52 ± 0.50. Finally, the rate of FRC increase (dFRC/dt) at the $1/40^{th}$ level was 2.0 ± 0.8 mL/s for N_2 and 3.1 ± 1.0 mL/s for Ar.

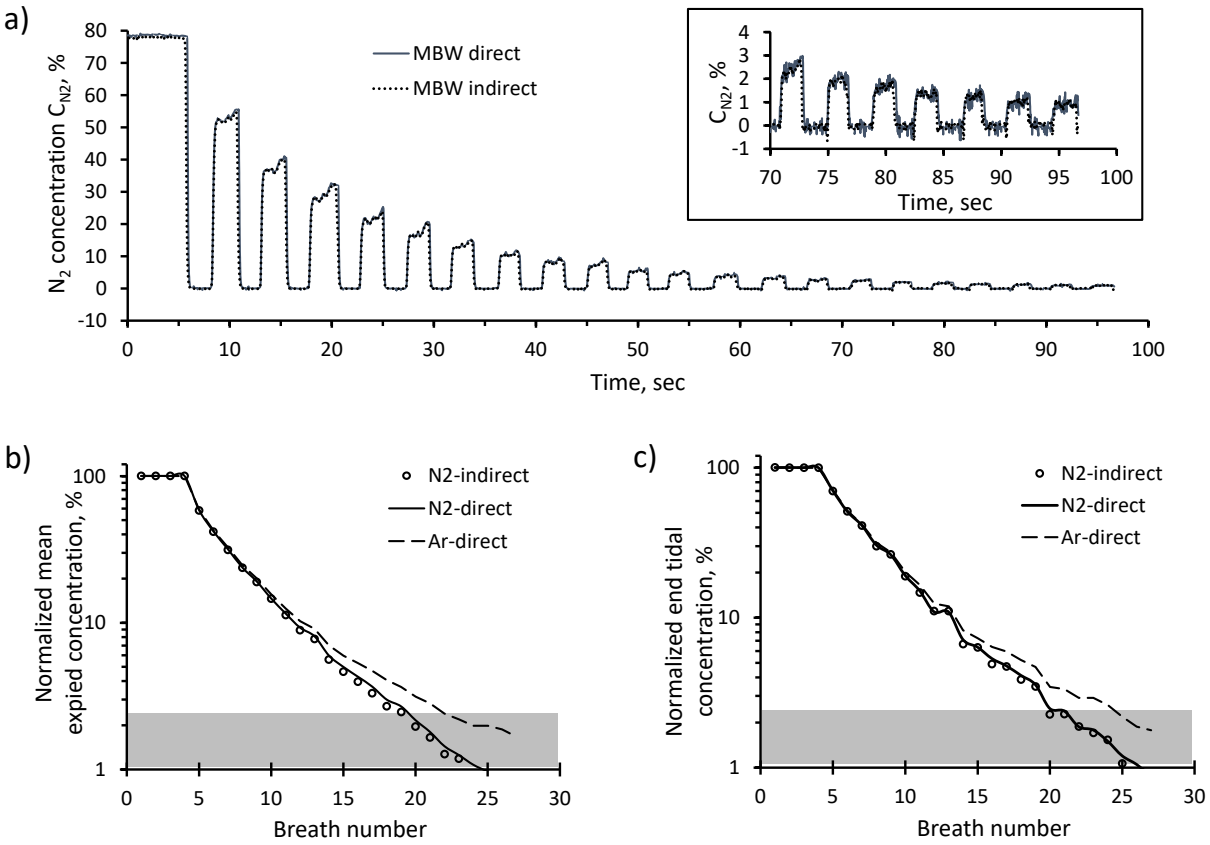

Figure 2. Raw N_2 concentration curves (panel a) and derived washout plots (panel b: mean expired N_2 concentration; panel c: end-tidal N_2 concentration) of a typical MBW test as measured by mass spectrometry (N_2-direct) and by the commercial device (N_2-indirect). Mean expired and end-tidal expired argon washout plots (Ar-indirect) are also shown in panels b and c, respectively, where all concentrations are normalized to pretest concentration with the grey area indicating concentration below 1/40th of pre-test concentration.

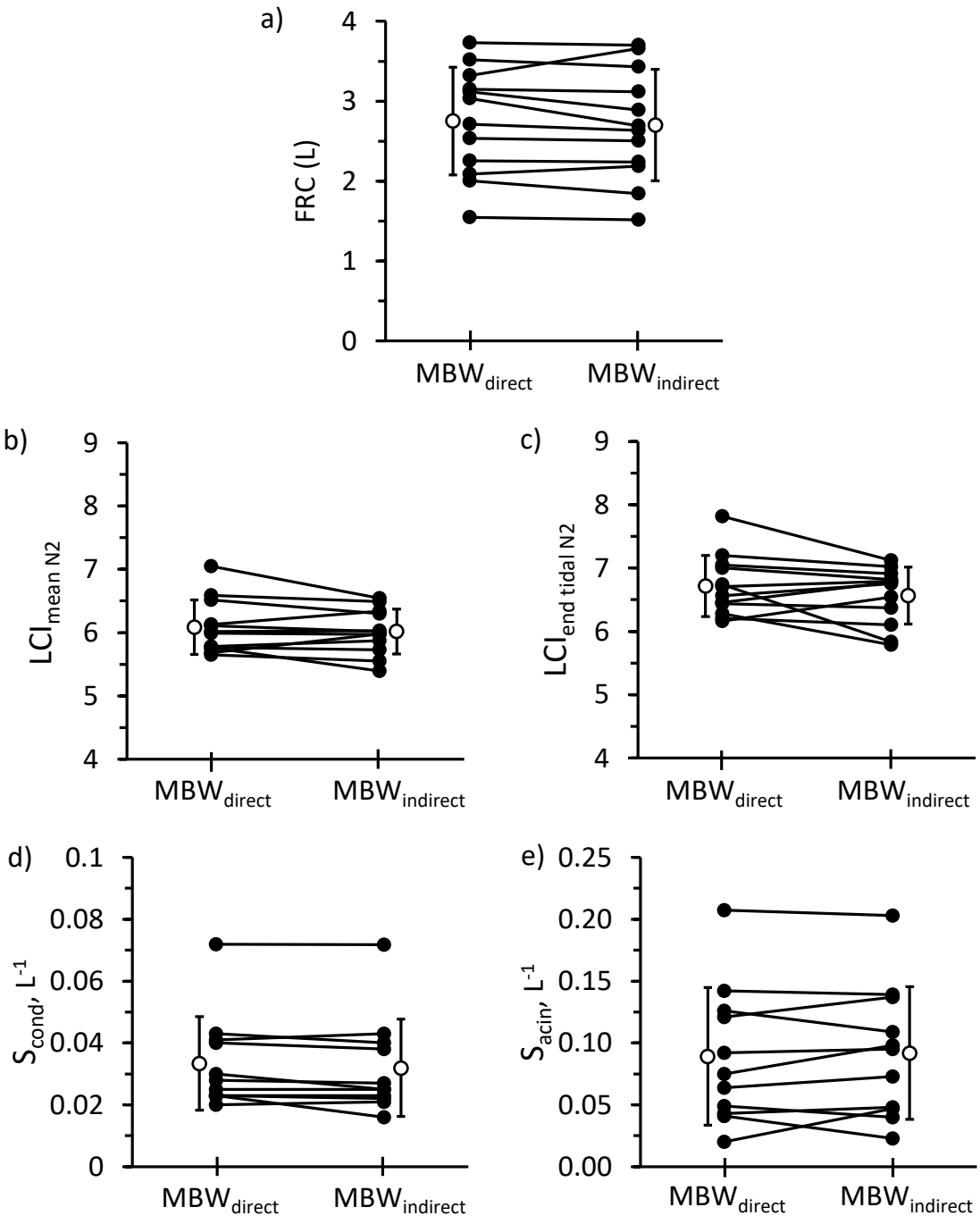

Figure 3. Comparison between MBW indices derived from data acquired by the mass spectrometer (MBW_{direct}) and by the commercial device ($MBW_{indirect}$): a) FRC, b) LCI derived from mean expired N_2 concentrations, c) LCI derived from end-tidal N_2 concentrations, d) S_{cond}, e) S_{acin}. Individual data are shown by solid symbols (•). Data averaged over all subjects (mean ± SD, n =12) are shown by open symbols.

Table1. Predicted N_2 concentrations in 2 compartments of the 3L lung model during 1L tidal breathing with 100% O_2.

						combined compartments 1&2				combined compartments 1&2				combined compartments 1&2			
		compartment 1		compartment 2		No soluble gas excretion				N_2 excretion (14)				Double N_2 excretion (14)			
Time	Breath	$C_{N2,1}$	$FRC_{estim,1}$	$C_{N2,2}$	$FRC_{estim,2}$	TO	C_{N2}	FRC_{estim}	$dFRC_{estim}/dt$	TO	C_{N2}	FRC_{estim}	$dFRC_{estim}/dt$	TO	C_{N2}	FRC_{estim}	$dFRC_{estim}/dt$
(s)	nb	(%)	(ml)	(%)	(ml)		(ml)	(%)	(ml/s)		(ml)	(%)	(ml/s)		(ml)	(%)	(ml/s)
0	0	78.0		78.0		0.00	78.0			0.00	78.0			0.00	78.0		
4	1	53.5	1200	62.4	1800	0.34	57.5	2804		0.33	57.9	2873		0.32	58.2	2945	
8	2	36.7	1200	49.9	1800	0.67	42.6	2831	6.5	0.66	43.0	2881	3.5	0.64	43.4	2932	0.3
12	3	25.1	1200	39.9	1800	1.01	31.8	2856	5.8	0.98	32.2	2901	5.2	0.96	32.5	2947	4.5
16	4	17.2	1200	31.9	1800	1.34	23.9	2878	5.1	1.31	24.2	2923	5.2	1.28	24.5	2968	5.2
20	5	11.8	1200	25.6	1800	1.68	18.0	2897	4.5	1.64	18.3	2943	4.8	1.60	18.7	2989	5.2
24	6	8.1	1200	20.4	1800	2.01	13.7	2914	3.9	1.97	14.0	2961	4.4	1.91	14.3	3009	4.9
28	7	5.6	1200	16.4	1800	2.35	10.4	2928	3.3	2.29	10.7	2978	3.9	2.23	11.1	3028	4.6
32	8	3.8	1200	13.1	1800	2.68	7.99	2940	2.8	2.62	8.30	2993	3.5	2.55	8.62	3046	4.2
36	9	2.6	1200	10.5	1800	3.02	6.15	2951	2.4	2.95	6.46	3006	3.1	2.87	6.77	3062	3.8
40	10	1.8	1200	8.4	1800	3.35	4.75	2960	2.0	3.28	5.06	3018	2.7	3.19	5.37	3077	3.5
44	11	1.2	1200	6.7	1800	3.69	3.69	2967	1.7	3.60	3.99	3028	2.4	3.51	4.29	3090	3.2
48	12	0.8	1200	5.4	1800	4.02	2.88	2973	1.4	3.93	3.17	3037	2.2	3.83	3.46	3102	2.9
52	13	0.6	1200	4.3	1800	**4.36**	**2.25**	**2978**	**1.1**	4.26	2.54	3045	1.9	4.15	2.82	3113	2.7
56	14	0.4	1200	3.4	1800	**4.69**	**1.76**	**2982**	**0.9**	**4.59**	**2.05**	**3053**	**1.7**	**4.47**	**2.33**	**3124**	**2.5**
60	15	0.3	1200	2.7	1800	5.03	1.38	2985	0.8	**4.91**	**1.66**	**3059**	**1.5**	**4.79**	**1.94**	**3133**	**2.3**
64	16	0.2	1200	2.2	1800	5.37	1.09	2988		5.24	1.36	3065		5.11	1.64	3142	

nb: number, TO: turnover (based on FRC from first breath below 1/40th level); bold numbers in grey areas indicate the breaths bracketing the 1/40th level of 78% initial concentration (i.e., 1.95% N_2).

Table 1 shows an example of simple dilution of a perfectly mixed gas with an initial C_{N2} at 78% in a two–compartment model with a specific ventilation of one compartment double that of the other one. Corresponding concentration curves versus lung turnover (Figure 4a) and estimated FRC (FRC_{estim}) curves versus time (Figure 4b) illustrate the effect of N_2 excretion and the impact of the presence of ventilation heterogeneity. Similar predictions were also obtained in the absence of ventilation heterogeneity (Figures 4c and 4d). In the homogeneous case, FRC_{estim} corresponds to the actual FRC of the model and $dFRC_{estim}/dt$ is zero in the absence of added gas excretion from blood-tissues. With the addition of a soluble gas at a rate provided by Lundin for N_2 (18) and at twice that rate (i.e. at a rate similar to that expected for argon), both FRC_{estim} and

$dFRC_{estim}/dt$ increase but the latter does not necessarily increase in proportion to excretion rate.

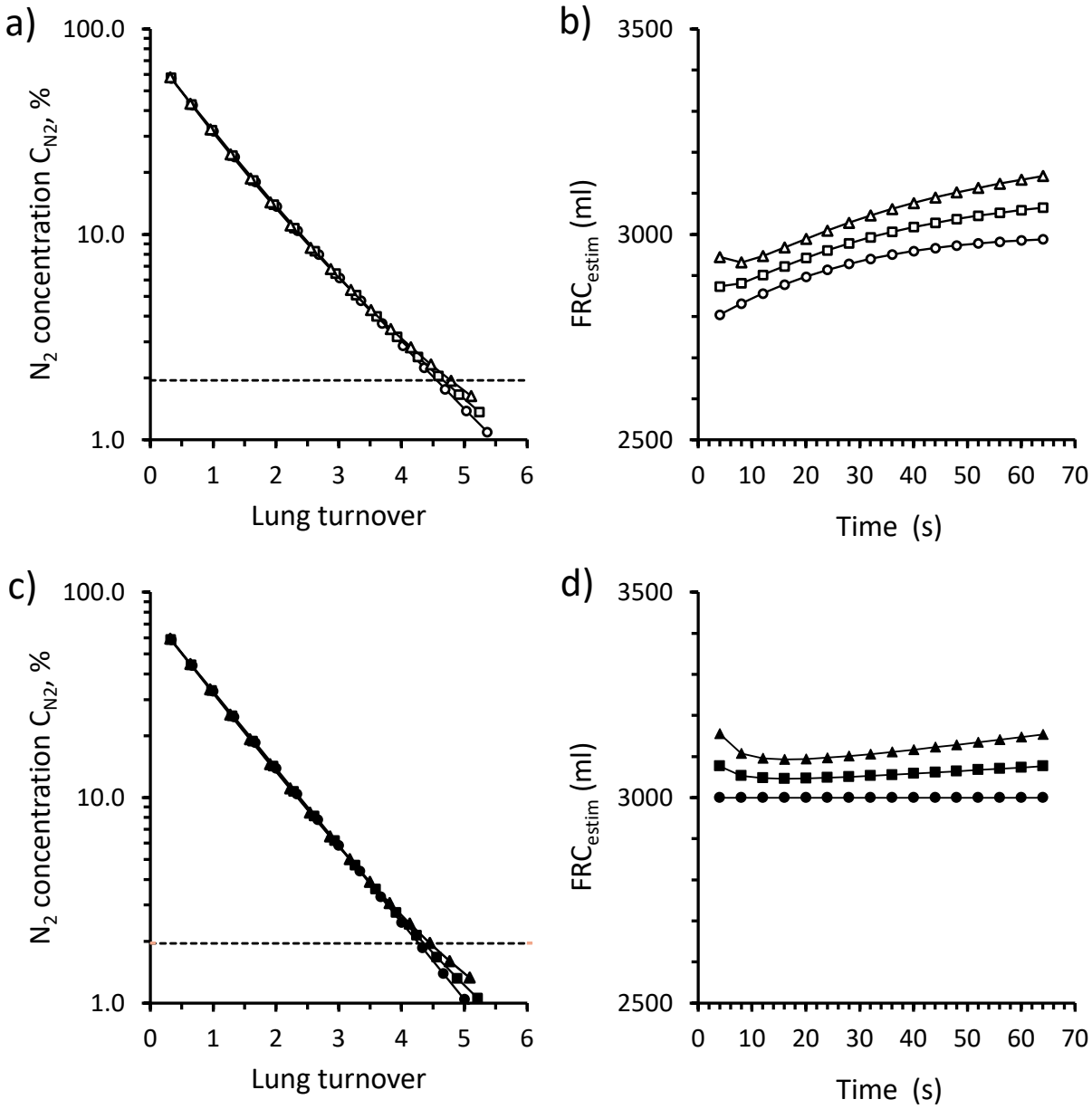

Figure 4. Dilution curves of N_2 concentration versus lung turnover (panels a,c) and estimated FRC (FRC_{estim}) versus time (panels b,d) for a homogeneously ventilated lung (panels c,d) and a heterogeneously ventilated one (panels a,b with corresponding numbers shown in Table 1); open symbols: heterogeneous model, closed symbols: homogeneous model. Each panel shows simulations assuming no gas excretion from blood and tissue (circles); gas excretion at a rate according to Lundin (18) (squares) and at twice that rate (triangles).

DISCUSSION

When the lung clearance index was first introduced as a physiological measurement in the 1950s, it was based on direct N_2 measurement (19, 20). Despite being acknowledged as a sensitive marker of ventilation distribution, routine clinical use of LCI has been hampered by the high cost or complexity of direct gas measurement techniques. Over the past decades, the availability of affordable and easy-to-use commercial devices based on indirect N_2 measurement has led to a regained interest in the use of LCI in clinical applications. However, it has been suggested that indirect N_2 measurement and N_2 stored in blood-tissue could both perturb and invalidate N_2-based LCI measurement (3). The present experimental data indicate otherwise. The excellent agreement between N_2 data from our commercial device and mass spectrometry (Figure 2) suggests that it is possible to obtain valid N_2-based MBW tests for LCI monitoring in the clinic. Importantly, experimental LCI values obtained here with N_2 or with twice as soluble Argon also indicates that the maximum impact from blood-tissue represents less than half a LCI unit in normal subjects.

Indirect N_2 calculation, while attractive, relies heavily on the accuracy of oxygen and CO_2 measurements as small errors in C_{O2} and C_{CO2} can result in significant error in C_{N2}, in particular towards the tail end of the test, which is critical to LCI determination particularly in disease (5, 6, 21). Recent studies using the EXHALYZER D® (Eco Medics, Duernten, Switzerland) showed markedly improved accuracy of FRC and LCI from N_2 MBW data when the interaction between CO_2 and O_2 sensors was corrected for, based on calibrated CO_2 and O_2 gas mixtures (21, 22). This correction removed a technical offset error that artificially prolonged the washouts, an issue that

is exacerbated by disease with long washout tails. While the device used here (EasyOne proLAB™) does account for the O_2 sensitivity of the CO_2 sensor which is used in addition to the molar mass ultrasonic sensor, our group has recently identified that accuracy of indirect N_2 measurement greatly benefits from the use of molar mass values based on calibration gas measurements rather than theoretical values (23). Since we obtain excellent agreement with mass spectrometry over the entire concentration range (down to low concentrations), longer washout tails in diseased patients will also be properly captured. Depending on the lung disease at hand, one could imagine the blood and/or tissue compartment to be affected, resulting in an altered uptake of soluble gases. To test this, the use of Argon as laid out in this work could be helpful, ideally complemented by an independent assessment of the blood-tissue compartment itself.

The impact of N_2 excreted from blood and tissue on FRC and LCI has been a matter of concern. Simple dilution calculations described in Table 1 and Figure 4 indicate that FRC and the resulting LCI are overestimated by gas excreted from blood and tissues, and that this overestimation partly depends on the presence of ventilation heterogeneity. Nielsen et al (10) performed more elaborate simulations in a two-compartment lung model that also included assumptions about varying N_2 excretion rates from blood-tissues and muscle in each compartment (with matched perfusion and ventilation). With a dead space fraction of 0.3, their model predicted that blood-tissue excreted N_2 would overestimate FRC by 2% and LCI by 4.5% when considering homogeneous ventilation (10). Increases in dead space associated with lung disease would invariably result in greater predicted overestimation of FRC and LCI (with a

maximum of 7% error in LCI for a dead space fraction of 0.85), while the predicted effect of ventilation heterogeneity was biphasic, with a maximum of ~5% in the mid-range.

While model assumptions about the N_2 gradients in different lung compartments are extremely difficult to verify experimentally, these simulations are nevertheless useful to interpret the experimental data. If we were to neglect the 1.2 greater diffusivity of N_2 versus argon, and attribute the difference between our experimental LCI_{Ar} and LCI_{N2} values entirely to gas solubility, then the 0.43 difference between LCI_{Ar} and LCI_{N2} (i.e., 6.52-6.09) amounts to an overestimation of 7% (=0.43/6.09). Similarly, if we consider that the 130ml difference between FRC_{N2} and FRC_{Ar} (= 2.87 L - 2.74 L) is solely due to argon being twice as soluble as N_2, one could speculate that the real FRC is at 2.61 L (= 2.74 L - 0.13 L), which comes down to a 5% error on FRC (=0.13/2.61). While some components of soluble gas-induced error will compensate each other (e.g., an overestimated FRC will attenuate the LCI overestimation) others will be a rather unpredictable balance between the contribution from the less ventilated N_2-rich compartments, which prolong the MBW washout but where the blood-gas N_2 gradient is reduced, and the better ventilated ones with larger blood-gas N_2 gradient.

The success of LCI determination hinges on good measurement accuracy towards the tail end of the washout plot, where concentrations are low. It has sometimes been suggested that beyond the $1/40^{th}$ threshold, the estimate of FRC should no longer increase, and that if it does, this is a sign of erroneous measurement (6). However, the dilution data in Table 1 and Figure 4b clearly show that the mere presence of ventilation heterogeneity representative of gravity-

dependent specific ventilation between upper and lower lung regions, leads to a $dFRC_{estim}/dt$ at the $1/40^{th}$ threshold of approximately 1 ml/s. Taken together with the experimental $dFRC_{estim}/dt$ of 2mL/s for N_2 and of 3mL/s of Ar, this implies that the portion of $dFRC_{estim}/dt$ attributable to N_2 excreted from blood and tissue is probably about 1ml/s, a value consistent with predictions retrieved from early literature (11).

For use as a physiological parameter in the clinic, the key message from our experimental data is in line with that of earlier reports, which acknowledge a contribution of blood-tissue N_2 but consider its maximal effect to be small enough and its actual effect too unpredictable, to recommend correcting for it (9, 11, 24). Considering the Ar washout, where LCI is already expected to be slightly greater due to the slightly less diffusive Ar - proportional to inverse square root of 40 g/mol (Ar) vs. 28 g/mol (N_2) - the combined effect of diffusion with that from blood-tissue Ar, sets an upper limit for blood-tissue contribution. In an effort to align LCI outputs from different MBW devices, the mismatch between LCI for different diffusivity gases, e.g. (21), is sometimes viewed as a measure of mismatch between devices. This may not be strictly true since simultaneous He and SF_6 washouts have shown distinct diffusion-dependent differences between these gases in normal subjects (25, 26) and the cross-over point between He and SF_6 washout curves has even been proposed as a diagnostic parameter to detect smoking-induced lung changes (8, 27).

In addition to gas diffusive properties and blood solubility, washout curves and their associated LCI can be affected by whether exogenous gases such as SF_6 are fully and

homogeneously washed in prior to washout. An exogeneous gas washin procedure has been proposed involving closed circuit rebreathing with CO_2 scrubbing (12) to attenuate this effect, but the corresponding simulations also showed that equilibration of gas concentration measured at the mouth may still correspond to considerable residual concentration heterogeneities inside the lungs. In such a case, the subsequent washout may be faster than it would have been in case of homogeneous test gas distribution at onset of washout, thus underestimating true LCI.

In conclusion, the potential impact of indirect measurement of N_2 and of N_2 excretion from the blood on LCI has led to concerns regarding the validity and usefulness of N_2 MBW testing. Here we have demonstrated by direct measurement of N_2 and twice as soluble argon, that indirect N_2 measurement is valid and that N_2 solubility effect on LCI is small.

ACKNOWLEDGEMENT

This project was supported by grant 1R01HL135496 from the NHLBI at the NIH and by the Fund for Scientific Research-Flanders (FWO-Vlaanderen, Belgium).

COI statement: None of the authors disclose any conflict of interest.

REFERENCES

1. **Verbanck S, Van Muylem A, Schuermans D, Bautmans I, Thompson B, and Vincken W**. Transfer factor, lung volumes, resistance and ventilation distribution in healthy adults. *European Respiratory Journal* 47: 166-176, 2016.

2. **Trinkmann F, Maros M, Roth K, Hermanns A, Schafer J, Gawlitza J, Saur J, Akin I, Borggrefe M, Herth FJF, and Ganslandt T**. Multiple breath washout (MBW) testing using sulfur hexafluoride: reference values and influence of anthropometric parameters. *Thorax* 76: 380-386, 2021.

3. **Nielsen JG**. Lung clearance index: should we really go back to nitrogen washout? *European Respiratory Journal* 43: 655-656, 2014.

4. **Jensen R, Stanojevic S, Gibney K, Salazar JG, Gustafsson P, Subbarao P, and Ratjen F**. Multiple Breath Nitrogen Washout: A Feasible Alternative to Mass Spectrometry. *Plos One* 8: e56868, 2013.

5. **Yammine S, Lenherr N, Nyilas S, Singer F, and Latzin P**. Using the same cut-off for sulfur hexafluoride and nitrogen multiple-breath washout may not be appropriate. *Journal of Applied Physiology* 119: 1510-1512, 2015.

6. **Guglani L, Kasi A, Starks M, Pedersen KE, Nielsen JG, and Weiner DJ**. Difference between SF_6 and N_2 multiple breath washout kinetics is due to N_2 back diffusion and error in N_2 offset. *Journal of Applied Physiology* 125: 1257-1265, 2018.

7. **Bayfield KJ, Horsley A, Alton E, Irving S, Bush A, and Davies JC**. Simultaneous sulfur hexafluoride and nitrogen multiple-breath washout (MBW) to examine inherent differences in MBW outcomes. *Erj Open Research* 5: 00234-02018, 2019.

8. **VonNieding G, Lîllgen H, Smidt U, and Lind H**. Simultaneous washout of helium and sulphur hexafluoride in healthy subjects and patients with chronic bronchitis, bronchial asthma and emphysema. *American Review of Respiratory Disease* 116: 649-660, 1977.

9. **Harris EA, and Whitlock RML**. Correction of inert gas washin or washout for gas solubility in blood. *Journal of Applied Physiology* 65: 1598-1603, 1988.

10. **Nielsen N, Nielsen JG, and Horsley AR**. Evaluation of the Impact of Alveolar Nitrogen Excretion on Indices Derived from Multiple Breath Nitrogen Washout. *PLOS ONE* 8: e73335, 2013.

11. **Kane M, Rayment JH, Jensen R, McDonald R, Stanojevic S, and Ratjen F**. Correcting for tissue nitrogen excretion in multiple breath washout measurements. *Plos One* 12: e0185553, 2017.

12. **Horsley AR, O'Neill K, Downey DG, Elborn JS, Bell NJ, Smith J, and Owers-Bradley J**. Closed circuit rebreathing to achieve inert gas wash-in for multiple breath wash-out. *ERJ Open Research* 2: 00042-02015, 2016.

13. **Robinson PD, Latzin P, Verbanck S, Hall GL, Horsley A, Gappa M, Thamrin C, Arets HGM, Aurora P, Fuchs SI, King GG, Lum S, Macleod K, Paiva M, Pillow JJ, Ranganathan S, Ratjen F, Singer F, Sonnappa S, Stocks J, Subbarao P, Thompson BR, and Gustafsson PM**. Consensus statement for inert gas washout measurement using multiple- and single-breath tests. *European Respiratory Journal* 41: 507-522, 2013.

14. **Bates JHT, Prisk GK, and McKinnon AE**. Correcting for the dynamic response of a respiratory mass spectrometer. *Journal of Applied Physiology* 55: 1015-1022, 1983.

15. **ndd Medical Technologies**. EasyOne Pro LAB Measurement Technology Background https://nddmed.com/_Resources/Persistent/80d9a89e4a98e093ecaf964ce55e02d83bea9ea1/AppNote-EOPLAB-TechBackground-V13R.pdf. [February 28, 2022].

16. **Oestreich M-A, Wyler F, Etter B, Ramsey KA, and Latzin P**. A non-systematic signal-correction error in a commercial multiple-breath washout device significantly impacts outcomes in children and adults. *medRxiv* 2022 (doi: 10.1101/2022.01.27.22269250).

17. **Verbanck S, Schuermans D, Van Muylem A, Paiva M, Noppen M, and Vincken W**. Ventilation distribution during histamine provocation. *Journal of Applied Physiology* 83: 1907-1916, 1997.

18. **Lundin G**. Nitrogen elimination during oxygen breathing. *Acta Physiologica Scandinavica Supplementum* 111: 130-143, 1953.

19. **Becklake MR**. A New Index of the Intrapulmonary Mixture of Inspired Air. *Thorax* 7: 111-116, 1952.

20. **Bouhuys A, and Lundin G**. Distribution of inspired gas in lungs. *Physiological Reviews* 39: 731-750, 1959.

21. **Sandvik RM, Gustafsson PM, Lindblad A, Robinson PD, and Nielsen KG**. Improved agreement between N2 and SF6 multiple breath washout in healthy infants and toddlers with improved EXHALYZER D® sensor performance. *Journal of Applied Physiology* 131: 107-118, 2021.

22. **Wyler F, Oestreich M-A, Frauchiger BS, Ramsey KA, and Latzin P**. Correction of sensor crosstalk error in Exhalyzer D multiple-breath washout device significantly impacts outcomes in children with cystic fibrosis. *Journal of Applied Physiology* 131: 1148-1156, 2021.

23. **Darquenne C, Theilmann RJ, and Verbanck S**. Improved Accuracy of Multiple Breath Nitrogen Washout Tracings Based on Indirect Molar Mass Measurements. *Am J Respir Crit Care Med* 201: A2998, 2020.

24. **Crawford ABH, Makowska M, Paiva M, and Engel LA**. Convection-and diffusion-dependent ventilation maldistribution in normal subjects. *Journal of Applied Physiology* 59: 838-846, 1985.

25. **Lacquet LM, Van Der Linden LP, and Paiva M**. Transport of H_2 and SF_6 in the lungs. *Respiration Physiology* 25: 157-173, 1975.

26. **Kawashiro T, Sikand RS, Adaro F, Takahashi H, and Piiper J**. Study of intrapulmonary gas mixing in man by simultaneous washout of helium and sulfur hexafluoride. *Respiration Physiology* 28: 261-275, 1976.

27. **DeVries WR, Luijendijk SCM, and Zwart A**. Helium and sulphur hexafluoride washout-in asymmetrical lung models. *Journal of Applied Physiology* 51: 1122-1130, 1981.

FIGURE LEGENDS

Figure 1. Alignment of gas concentration traces from the mass-spectrometer (MBW_{direct}) and the commercial device ($MBW_{indirect}$) by matching the C_{CO2} at 50% of maximal C_{CO2} in the transition from the first expiration of the MBW test to the next inspiration (see arrow).

Figure 2. Raw N_2 concentration curves (panel a) and derived washout plots (panel b: mean expired N_2 concentration; panel c: end-tidal N_2 concentration) of a typical MBW test as measured by mass spectrometry (N_2-direct) and by the commercial device (N_2-indirect). Mean expired and end-tidal expired argon washout plots (Ar-indirect) are also shown in panels b and c, respectively, where all concentrations are normalized to pretest concentration with the grey area indicating concentration below 1/40th of pre-test concentration.

Figure 3. Comparison between MBW indices derived from data acquired by the mass spectrometer (MBW_{direct}) and by the commercial device ($MBW_{indirect}$): a) FRC, b) LCI derived from mean expired N_2 concentrations, c) LCI derived from end-tidal N_2 concentrations, d) S_{cond}, e) S_{acin}. Individual data are shown by solid symbols (•). Data averaged over all subjects (mean ± SD, n =12) are shown by open symbols.

Figure 4. Dilution curves of N_2 concentration versus lung turnover (panels a,c) and estimated FRC (FRCestim) versus time (panels b,d) for a homogeneously ventilated lung (panels

c,d) and a heterogeneously ventilated one (panels a,b with corresponding numbers shown in Table 1); open symbols: heterogeneous model, closed symbols: homogeneous model. Each panel shows simulations assuming no gas excretion from blood and tissue (circles); gas excretion at a rate according to Lundin (18) (squares) and at twice that rate (triangles).